Journal of Power Sources 231 (2013) 91–96

Contents lists available at SciVerse ScienceDirect

Journal of Power Sources

journal homepage: www.elsevier.com/locate/jpowsour

Short communication

High crystallinity binuclear iron phthalocyanine catalyst with enhanced performance for oxygen reduction reaction

Xiaoming Hu [b], Dingguo Xia [a,*], Lei Zhang [c], Jiujun Zhang [c,**]

[a] College of Engineering, Peking University, Beijing 100871, PR China
[b] College of Environmental & Energy Engineering, Beijing University of Technology, Beijing 100022, PR China
[c] NRC Energy, Mining & Environment Portfolio, National Research Council, Vancouver, BC V6T 1W5, Canada

HIGHLIGHTS

- High crystallinity binuclear iron phthalocyanine was synthesized.
- The bi-FePc/MWNT catalyst exhibits a superior electrochemical performance.
- The stacking axis of the bi-FePc molecules is parallel to the substrate.

ARTICLE INFO

Article history:
Received 4 August 2012
Received in revised form
3 December 2012
Accepted 5 December 2012
Available online 24 December 2012

Keywords:
High crystallinity
Binuclear iron phthalocyanine
Oxygen reduction reaction
Multi-walled carbon nanotubes

ABSTRACT

High crystallinity binuclear iron phthalocyanine coated onto multi-walled carbon nanotubes (bi-FePc/MWNT), was synthesized. Transmission electron microscopy (TEM) confirms that the crystalline bi-FePc forms a uniform coating on the carbon nanotubes with a thickness of about 20 nm. The plane of the macrocyle is perpendicular to the surface of the nanotube and the stacking axis of the bi-FePc molecules, which is the direction of high electrical conductivity, is found to be parallel to the substrate. The bi-FePc/MWNT show activity of 1.43 mA cm^{-2} at 0.66 V versus NHE indicating good activity and the current is stable for 14 h as electrocatalyst in oxygen reduction reactions (ORR) indicating good stability; the oxygen reduction current does not change in the presence of methanol showing the binuclear iron phthalocyanine coated onto multi-walled carbon nanotubes specifically catalyzes oxygen reduction and not methanol oxidation.

© 2012 Elsevier B.V. All rights reserved.

1. Introduction

Direct methanol fuel cells (DMFC's) are promising technologies for portable electronics applications such as cellular phones, personal digital assistants, and laptop computers, due to the transpiration properties of liquid methanol and its ease of storage [1]. However, Pt-based catalysts for both the methanol oxidation reaction (MOR) at the anode and the oxygen reduction reaction (ORR) at the cathode present major challenges, hindering the commercialization of DMFC technology. These challenges include the catalysts' high cost, poor stability, and an intolerance to methanol crossover [2–5]. As a result, some alternative catalysts that are based on non-noble metals have been the object of intense research for the past several decades, because they are less expensive and generally methanol tolerant. In the effort to develop non-noble metal catalysts, the use of transition metal macrocyclic or phthalocyanine compounds has been a promising approach, ever since Jasinski's discovery of their catalytic activity in oxygen reduction reactions [6]. Unfortunately, while most of the metallophthalocyanines and metalloporphyrins have been found to exhibit a good initial oxygen reduction performance [7–9], their stability calls for some improvement [10]. The decomposition via hydrolysis in an electrolyte, or an attack by peroxide intermediates on macrocycle rings, are known to be the main causes of the poor stability. Although pyrolyzed transition metal-containing macrocycle catalysts exhibit both an improved ORR activity as well as good stability [6,11], these improved properties are still insufficient to allow for use in DMFC applications. Recently, Zelenaya et al. have described a novel synthesis method for catalysts containing iron and cobalt that exhibit even better activity and stability properties [12–15]. In this work, we report on a novel non-precious electrocatalyst with a high ORR activity and good stability, which is also inexpensive to produce. This catalyst is a carbon nanotube induced binuclear Fe-

* Corresponding author. Tel.: +86 10 82529046; fax: +86 10 82529010.
** Corresponding author. Tel./fax: +1 604 221 3087.
E-mail addresses: dgxia@pku.edu.cn (D. Xia), jiujun.zhang@nrc.gc.ca (J. Zhang).

0378-7753/$ – see front matter © 2012 Elsevier B.V. All rights reserved.
http://dx.doi.org/10.1016/j.jpowsour.2012.12.018

phthalocyanine material with high crystallinity. Even without heat treatment, the new catalyst was shown to have superior ORR activity levels and enhanced stability properties, as well as a high methanol tolerance.

2. Experimental procedure

The carbon nanotube induced, high crystallinity binuclear iron phthalocyanine (bi-FePc/MWNT) was synthesized for the first time using a solvent thermal process. In a typical process, 512 mg of dicyanobenzene, 179 mg of tetracyanobenzene, and 219 mg of $FeCl_2 \cdot 4H_2O$ were dissolved in 25 ml of quinoline (under stirring) to form a precursor solution. This solution was then slowly added to a suspension of MWNT, forming a mixture between the MWNT and the precursor. The suspension containing MWNT was pre-prepared by mixing 106 mg of MWNT in a quinoline solvent, subject to sonication in an ultrasonic bath for 15 min. The mixture was then stirred at 200 °C under nitrogen for 4 h, and subsequently filtered, washed with ethanol, and dried in vacuum at 80 °C for 24 h.

For comparison of the performance of the final product in catalyzed oxygen reduction reactions, an amount of bi-FePc without MWNT support was also synthesized using the same procedure.

For particle characterization, high-resolution transmission electron microscopy (HRTEM) images and electron diffraction data were collected on a JEOL JEM-2010F. Optical absorption spectra were also recorded using a Hitachi U-3010UV/Vis/NIR Spectrometer, and infrared (IR) spectra were acquired in the range of 1550–1100 cm^{-1} with a Digilab FTS7000 spectrometer.

To characterize the electrochemical properties of the material, we performed cyclic voltammetry (CV) and rotating disc electrode (RDE) measurements using a three-electrode electrochemical cell in a 0.5 M H_2SO_4 solution. The working electrode (rotating glassy-carbon disk electrode with a geometric area of 0.126 cm^2) was prepared by pipetting a controlled amount of bi-FePc/MWNT & Nafion® ink onto the electrode surface to form a thin layer of Nafion®-bonded catalyst. The mixture of bi-FePc/MWNT & Nafion® ink was in turn prepared by ultrasonically mixing the bi-FePc/MWNT in a Nafion® ionomer solution (5% in alcohol), in a ratio of 90:10 wt%, for 10 min. Another electrode was coated with bi-FePc mixed with XC-72, where the same manufacturing procedure was used. A standard hydrogen electrode and glass carbon electrode were used as the reference and the auxiliary electrodes, respectively. We performed electrochemical measurements using an EG&G Model 273A potentiostat/galvanostat, controlled by M270 software. All experiments were conducted at room temperature and ambient pressure.

3. Results and discussion

3.1. Confirmation of bi-FePc/MWNT formation using visible spectroscopy

In order to confirm the formation of bi-FePc/MWNT, we obtained visible absorption spectra of bi-FePc/MWNT and the unsupported bi-FePc in a dimethyl sulfoxide (DMSO) solution. The spectra are shown in the Supporting information section in Figure S1. For both substances, the Soret and Q bands are observed. In particular, a shoulder in the spectra, close to the Q band, can be attributed to a transition involving a vibrational excited state [16]. While the spectra for both bi-FePc/MWNT and bi-FePc are similar in terms of band positions, and the Q bands for both substances appear at the same energy, the Soret band is shifted to higher energies for bi-FePc/MWNT when compared to the case of bi-FePc. This suggests that the energy of the highest unoccupied molecular orbital (HUMO) is the same for both bi-FePc and bi-FePc/MWNT, whereas that of the lowest occupied molecular orbital (LOMO) probably has a higher energy in bi-FePc/MWNT than in bi-FePc, resulting in a smaller HOMO–LUMO gap for bi-FePc/MWNT than the one for bi-FePc. This in turn means that bi-FePc/MWNT should be better able to donate electrons.

3.2. TEM observation of crystallinity in a bi-FePc layer on a MWNT

Shown in Fig. 1 are TEM images of bi-FePc/MWNT and unsupported bi-FePc. In the presence of MWNT, one can see that the crystalline bi-FePc is coated uniformly onto a carbon nanotube with a thickness of about 20 nm. In the high-resolution the TEM image shown in Fig. 1(b), lattice fringes can be clearly observed. The observed crystal lattices have an interplanar spacing of 1 nm, which is quite close to what is expected for (211) planes for bi-FePc, providing further evidence that the nano-coating seen in Fig. 1(b) consists of the high-crystallinity phase of bi-FePc. The crystalline bi-FePc on the surface of a MWNT appears to grow in a direction that is parallel to the substrate surface, i.e., the stacking axis (*b* axis) of the bi-FePc molecules, which is also the direction of high electrical conductivity, lies parallel to the substrate. In contrast, in the absence of MWNT support, the bi-FePc in solution is amorphous (as seen in Fig. 1(d)), and therefore that sample has a higher resistance, since many of the stacking axes are not parallel to any surface. Fig. 2 illustrates the underlying mechanisms for the formation of high crystallinity bi-FePc on the surface of a MWNT. The bi-FePc molecules are first absorbed along the interface of MWNT (Fig. 2(a)). Because of a $\pi-\pi$ interaction between bi-FePc molecules, a crystal is formed and grown with a preferred orientation of some crystal plane. When the single crystal grows to a certain extent, the stacking axes are no longer parallel but somewhat inclined, due to stress in the crystal (Fig. 2(b) and (c)). Since the physical properties of phthalocyanine compounds are largely influenced by their morphology and crystallinity [17], the high crystallinity and specific surface orientation in bi-FePc/MWNT should yield an improved level of electrochemical activity. Moreover, Inductive Coupled Plasma Emission Spectrometer (ICP) test shows the loading of bi-FePc on MWNT is 30% by weight. To the best of our knowledge, this paper is the first to report on high crystallinity bi-FePc/MWNT with specific surface orientation.

3.3. Catalytic activity of bi-FePc/MWNT in oxygen reduction reactions (ORR)

We measured and compared the ORR activity of bi-FePc/MWNT and unsupported bi-FePc. Fig. 3 shows the polarization curves as recorded on GC electrodes that were individually coated with each of the two catalysts in O_2-saturated 0.5 mol dm^{-3} H_2SO_4 electrolyte solution, in both the presence and absence of methanol. In the absence of methanol, for the bi-FePc/MWNT catalyst, an onset potential of 0.85 V vs. standard hydrogen electrode (SHE) can be observed, which is higher than that found for bi-FePc. It could be attributed an outstanding electronic conductivity of MWNT relative to the bi-FePc. Moreover, it is well known that transition metal N_4 chelates are inert to methanol. The insensitivity of the high crystallinity bi-FePc/MWNT catalyst to methanol is demonstrated in Fig. 3, where the ORR polarization curve is clearly not significantly affected by the presence of 0.5 M methanol in the electrolyte.

Fig. 4 shows cyclic voltammograms for a GC electrode coated with bi-FePc/MWNT in 0.5 mol dm^{-3} H_2SO_4 solution, saturated with either N_2 or O_2, respectively. In an N_2-saturated solution, the bi-FePc/MWNT exhibits a reversible redox wave that is located at about 0.45 V, which can be attributed to the redox reaction of bi-Fe(II)Pc/bi-Fe(III)Pc. When the solution is saturated with O_2, a large reductive peak at 0.66 V (vs. NHE) is observed, with a peak

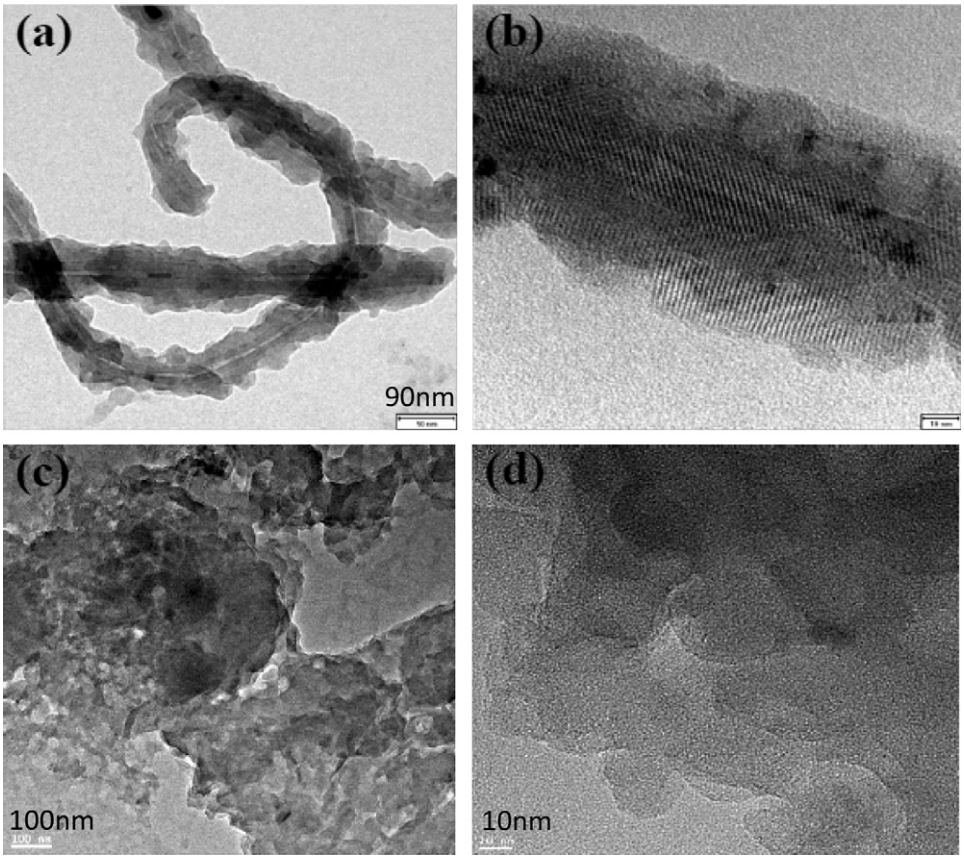

Fig. 1. TEM images of bi-FePc/MWNT (a, b) and bi-FePc (c, d) catalysts.

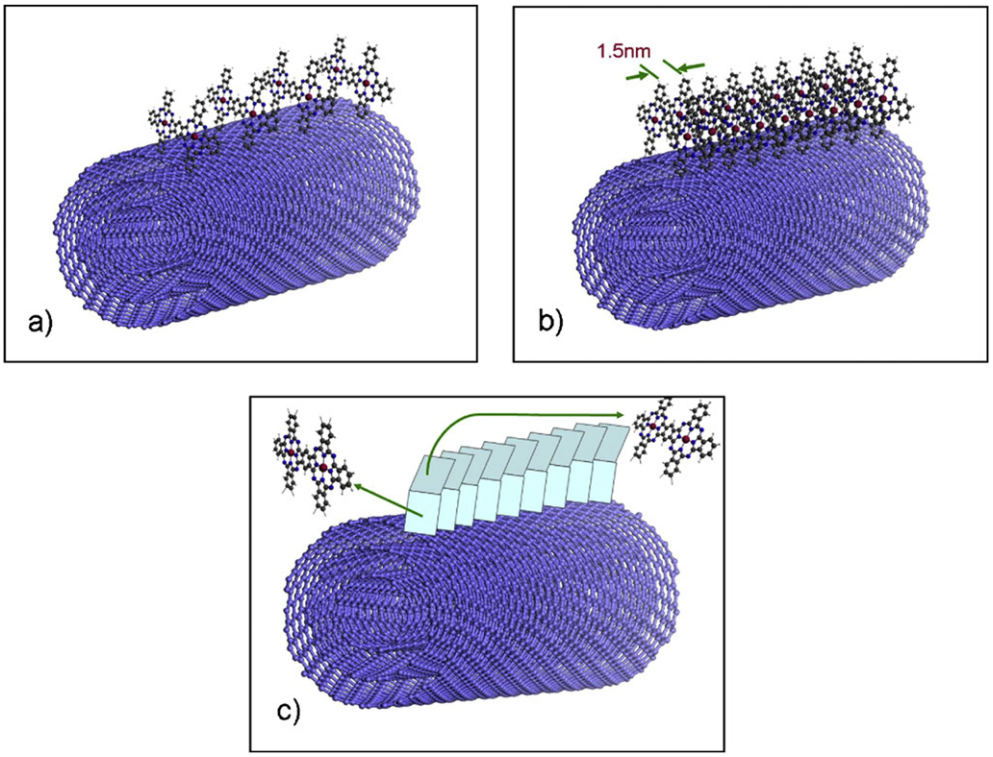

Fig. 2. Formation mechanisms for high crystallinity bi-FePc/MWNT.

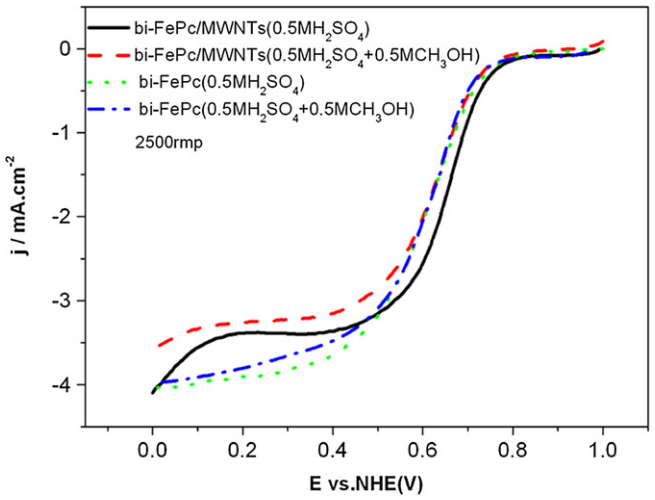

Fig. 3. ORR current–voltage curves obtained using rotating GC disk electrodes individually coated with bi-FePc/MWNT and bi-FePc catalysts, in O_2-saturated 0.5 M H_2SO_4 electrolyte in both the presence and absence of 0.5 M methanol. Electrode rotation rate: 2500 rpm S^{-1}. Potential scan rate: 10 mV s^{-1}. Loading of both bi-FePc/MWNT and bi-FePc: 5.3 mg cm^{-2}.

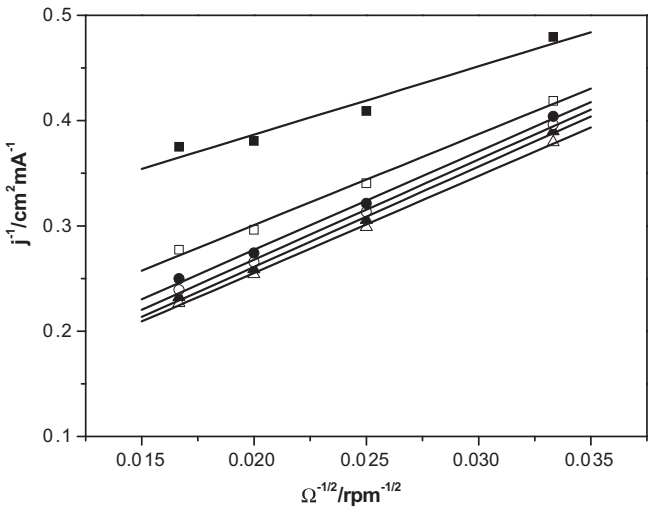

Fig. 5. Koutecký–Levich plots determined from Figure S2. Symbols: △ at electrode potentials of 565 mV, ▲ at 500 V, ○ at 430 mV, ● at 355 mV, □ at 300 mV, and ■ at 230 mV vs. RHE.

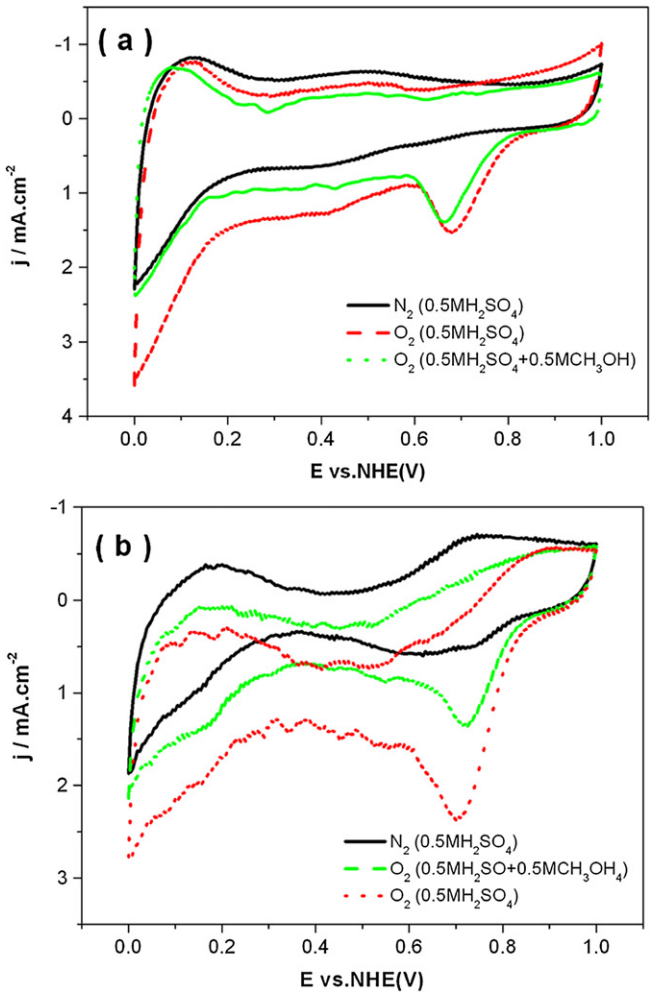

Fig. 4. Cyclic voltammograms of a GC electrode coated with bi-FePc (a) and bi-FePc/MWNT (b) in 0.5 M H_2SO_4 solution (saturated with N_2, O_2), and with 0.5 M CH_3OH solution (saturated with O_2). Potential scan rate: 20 mV s^{-1}. Loading of bi-FePc/MWNT: 5.3 mg cm^{-2}.

current of 1.43 mA cm^{-2} and an ORR onset potential of 0.85 V. With 0.5 M methanol in the solution, no methanol oxidation could be observed, indicating that the bi-FePc/MWNT catalyst is electrochemically resistant to methanol oxidation. As to the lower oxygen reduction current after methanol added, it may be contributed to the reducing of active sites due to the adsorption of methanol on the surface of catalyst. Similar experiments with pure Pt and other Pt-based catalysts, such as PtRu, PtFe, and PtNi, all showed that these catalysts have no such methanol tolerance [2,3,18]. As mentioned in the Introduction, one of the major challenges in DMFCs is found in the methanol crossover from anode to cathode, causing a depletion in the surface concentration of oxygen, poisoning of the cathode catalyst, and an accompanying reduction in fuel efficiency. It is therefore highly desirable to use a cathode catalyst that has no catalytic activity toward methanol oxidation. We believe that our bi-FePc/MWNT catalyst is a feasible candidate to serve as cathode catalyst in DMFCs, which could eliminate the negative effects of the methanol crossover.

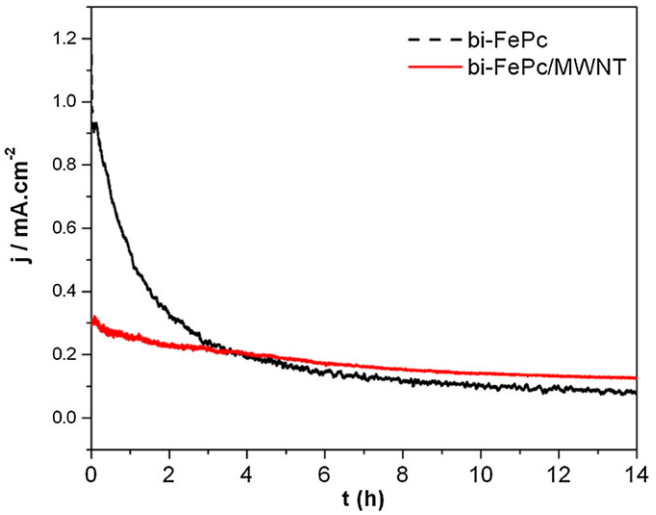

Fig. 6. Chronoamperometric curves of ORR catalyzed by bi-FePc/MWNT and bi-FePc, in O_2-saturated 0.5 M H_2SO_4 solution at an electrode potential of 0. 71 V vs. NHE. Loading of both bi-FePc/MWNT and bi-FePc: 5.308 mg cm^{-2}.

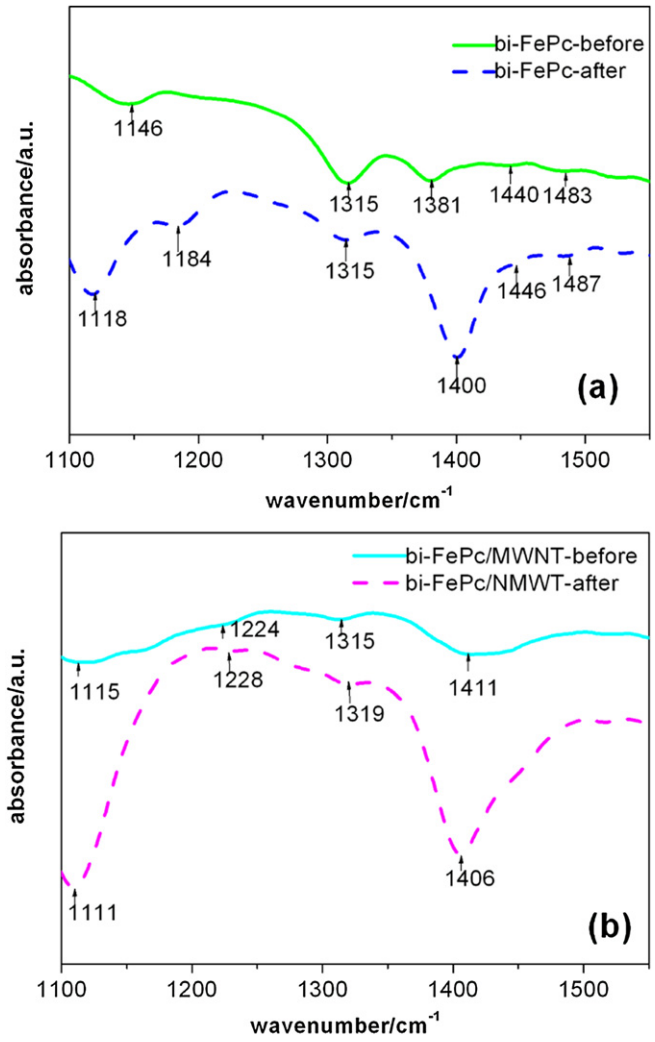

Fig. 7. IR spectra (20 °C) of (a) bi-FePc, and (b) bi-FePc/MWNT electrodes, recorded before and after 3 h of ORR testing in O_2-saturated 0.5 M H_2SO_4 solution.

The kinetic parameters of an ORR catalyzed by bi-FePc/MWNT were also investigated using a rotating disk electrode technique within an electrode rotation rate range of 400–2500 rpm. The polarization curves thus recorded, as well as plots of the reciprocal of the current density versus the reciprocal square root of the rotation rate, are shown in the Supporting information section (Figure S2). Using published data [19], the overall electron transfer number was calculated to be 3.8, based on the measured slope value shown in Fig. 5. This value is fairly close to 4, suggesting that the ORR catalyzed by bi-FePc/MWNT involves a 4-electron donation process from O_2 to water.

3.4. Catalyst stability in oxygen reduction reactions

To examine the ORR stability of both the bi-FePc/MWNT and bi-FePc catalysts, we conducted chronoamperometry tests at 0.71 V vs. NHE, and the results are shown in Fig. 6. In that figure, we see that the current density degrades rapidly in time from an initial value of 0.30 mA cm^{-2}, and reaches a steady current density of 0.07 mA cm^{-2} within 14 h. Compared with similar curves for unsupported bi-FePc, the steady current density catalyzed by bi-FePc/MWNT is higher, indicating that the bi-FePc/MWNT electrocatalyst has a greater stability than does bi-FePc.

3.5. Insight into stability enhancement

Regarding the degradation mechanism in chronoamperometry, Coutanceau et al. found that there was an absorption band located at ~1195 cm^{-1} after chronoamperometry [20], and proposed that the main degradation mechanism for FePc that occurs on an electrode should be the result of demetallization of the macrocycle. This hypothesis was confirmed when comparing the IR spectrum from an aged sample with that from commercial grade H_2Pc. After demetallization of the FePc catalyst, the remaining H_2Pc is no longer able to catalyze the ORR, indicated by the fact that it has no observable ORR activity [21,22]. Fig. 7 depicts IR spectra for bi-FePc (a) and bi-FePc/MWNT (b) before and after a 3-h chronoamperometry procedure in O_2-saturated 0.5 mol dm^{-3} H_2SO_4 solution. These measurements were carried out in the so-called fingerprint range of IR wavenumbers (1000–1500 cm^{-1}). The band located at 1184 cm^{-1} for bi-FePc matches the characteristic absorption band of H_2Pc, suggesting that demetallization of FePc during chronoamperometry is taking place [20]. However, for bi-FePc/MWNT, the before and after IR absorption bands for a 3-h chronoamperometry test are basically unchanged, except for a small decrease in intensity. Therefore, we can conclude that bi-FePc/MWNT possesses superior stability properties as a catalyst in an acid medium when compared with bi-FePc.

In order to fundamentally understand the improved stability of bi-FePc/MWNT over that of bi-FePc in ORR, the XPS spectra of the Fe 2p for these two catalysts are shown in Fig. 8. The Fe 2p signal derives from the contribution of two doublets. The main species can be related to the iron ion (Fe 2p3/2 line) with a binding energy of 710.61 eV and 709.86 eV for bi-FePc/MWNT and bi-FePc, respectively. The position of the XPS peaks for the iron ions in the bi-FePc/MWNT sample is upshifted by 0.75 eV with respect to the bi-FePc sample. This shift in the binding energy indicates that the

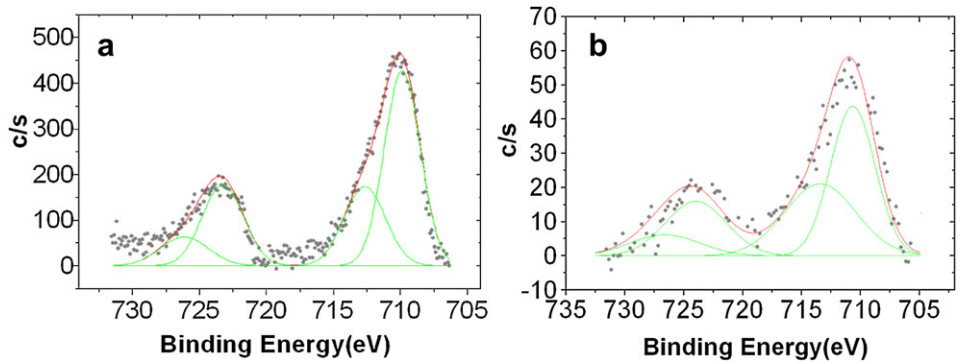

Fig. 8. XPS spectra for Fe 2p doublet in (a) bi-FePc, and (b) bi-FePc/MWNT.

bonding of iron ions with N_4 ligands in bi-FePc/MWNT is stronger than it is in bi-FePc, suggesting that bi-FePc/MWNT should be more stable than bi-FePc.

4. Conclusions

In summary, a carbon nanotube induced, high crystallinity planar binuclear iron phthalocyanine (bi-FePc/MWNT) was synthesized for the first time with an in-situ method. The bi-FePc was coated uniformly onto carbon nanotubes, with stacking axes parallel to the surface, with a thickness of about 20 nm. Experiments indicate that this novel bi-FePc/MWNT catalyst can catalyze a direct 4-electron reduction of oxygen to water. In comparison with an unsupported, amorphous bi-FePc catalyst, the bi-FePc/MWNT catalyst exhibits superior activity and enhanced stability. This new catalyst also has a good methanol tolerance, suggesting that its use in direct methanol fuel cell cathodes should result in the improved performance of such devices.

Acknowledgment

This work is financially supported by the Beijing Municipal Natural Science Foundation (No. 20110001) and the National Natural Science Foundation of China (No. 11179001).

Appendix A. Supplementary data

Supplementary data related to this article can be found at http://dx.doi.org/10.1016/j.jpowsour.2012.12.018.

References

[1] L. Zhang, J.J. Zhang, D.P. Wilkinson, H.J. Wang, J. Power Sources 156 (2006) 171–182.
[2] J.-F. Drillet, A. Ee, J. Friedemann, R. Kötz, B. Schnyder, V.M. Schmidt, Electrochim. Acta 47 (2002) 1983.
[3] A.K. Shukla, R.K. Raman, N.A. Choudhury, K.R. Priolkar, P.R. Sarode, S. Emura, R. Kumashiro, J. Electroanal. Chem. 563 (2004) 181.
[4] L. Dubau, C. Coutanceau, E. Garnier, J.-M. Léger, C. Lamy, J. Appl. Electrochem. 33 (2003) 419.
[5] C. Coutanceau, A.F. Rakotondrainibe, A. Lima, E. Garnier, S. Pronier, J.-M. Léger, C. Lamy, J. Appl. Electrochem. 34 (2004) 61.
[6] R. Jasinski, Nature 201 (1964) 1212.
[7] M. Savy, P. Andro, C. Bernard, G. Magner, Electrochim. Acta 18 (1973) 191.
[8] J. Zagal, P. Bindra, E. Yeager, J. Electrochem. Soc. 127 (1980) 1506.
[9] M.R. Tarasevich, A. Sadkowski, in: E. Yeager, B.E. Conway, J.O'M. Bockris, S.U.M. Khan, R.E. White (Eds.), Comprehensive Treatise of Electrochemistry, vol. 7, Plenum Press, New York, p. 301.
[10] C. Coutanceau, A. El Hourch, P. Crouigneau, J.M. Léger, C. Lamy, Electrochim. Acta 40 (1995) 2739.
[11] S. Gupta, D. Tryk, I. Bae, W. Aldred, E. Yeager, J. Appl. Electrochem. 19 (1989) 19.
[12] B. Pielaa, T.S. Olsonb, P. Atanassovb, P. Zelenaya, Electrochim. Acta 55 (2010) 7615–7621.
[13] D.A. Scherson, S.L. Gupta, C. Fierro, E.B. Yeager, M.E. Kordesch, J. Eldridge, R.W. Hoffman, J. Blue, Electrochim. Acta 28 (1983) 1205.
[14] J.A.R. Van Veen, H.A.Z. Colijn, J.F. Van Baar, Electrochim. Acta 33 (1988) 801.
[15] G. Lalande, G. Faubert, R. Côté, D. Guay, J.P. Dodelet, L.T. Weng, P. Bertrand, J. Power Sources 61 (1996) 227.
[16] M. Stillman, T. Nyokong, in: C.C. Lezno, A.B.P. Lever (Eds.), Phthalocyanines, vol. 1, VCH Publishers, U.S.A., 1993.
[17] C.Y. Wang, Chun-Pei Cho, Tsong-Pyng Perng, Thin Solid Films 518 (2010) 6720–6728.
[18] Xiang Li, Li An, X.Y. Wang, J. Mater. Chem. 22 (2012) 6047.
[19] R.C.M. Jakobs, L.J.J. Janssen, E. Barendrecht, Electrochim. Acta 30 (1985) 1085.
[20] S. Baranton, C. Coutanceau, C. Roux, F. Hahn, J.-M. Leger, J. Electroanal. Chem. 577 (2005) 223–234.
[21] J. Zagal, M. Paéz, A.A. Tanaka, J.R. dos Santos Jr., C.A. Linkous, J. Electroanal. Chem. 339 (1992) 13.
[22] J.P. Randin, Electrochim. Acta 19 (1974) 83.